

X-ray Variability of AGN and the Flare Model

R.W. Goosmann¹, B. Czerny², A.-M. Dumont¹, M. Mouchet¹,
and A. Różańska²

¹ *LUTH, Observatoire de Paris, Meudon, France*

² *Nicolaus Copernicus Astronomical Center, Warsaw, Poland*

Abstract. Short-term variability of X-ray continuum spectra has been reported for several Active Galactic Nuclei. Significant X-ray flux variations are observed within time scales down to $10^3 - 10^5$ seconds. We discuss short variability time scales in the frame of the X-ray flare model, which assumes the release of a large hard X-ray flux above a small portion of the accretion disk. The resulting observed X-ray spectrum is composed of the primary radiation and of a reprocessed Compton reflection component that we model with numerical radiative transfer simulations. The incident hard X-rays of the flare will heat up the atmosphere of the accretion disk and hence induce thermal expansion. Eventually, the flare source will be surrounded by an optically -thick medium, which should modify the observed spectra.

1. Introduction

In the last few years several Active Galactic Nuclei (AGN) showing short-term X-ray variability have been reported (see for instance Ark 564 and Ton S180 (Edelson et al. 2002), I Zw 1 (Gallo et al. 2004), MGC-6-30-15 (Vaughan & Fabian 2004; Ponti et al. 2004)). Modeling this behavior remains a complex task: owing to the short variability time scales observed, one has to assume small emission regions down to the size of a few R_{Schw} (Schwarzschild radii). Such regions exist within the framework of the flare model. In this model compact hard X-ray sources resulting from magnetic reconnection evolve above the accretion disk.

In the following we present detailed numerical modeling of the reprocessed X-ray spectra induced by a magnetic flare. We investigate the influence of a realistic flare illumination as compared to an isotropic one and the dependency on the disk inclination. Using this model we attempt to derive the consequences for the time evolution of the observed spectra.

Then we briefly discuss the hydrostatic balance and the optical properties of a the disk atmosphere below a flare.

2. The composite spectrum of a flare-irradiated hot-spot

2.1. Modeling

We assume a plane-parallel model atmosphere at a typical distance of $9R_{Schw}$ from the central black hole. Collin et al. (2003) have shown that, after the onset of a flare, the thermal and the ionization profile change much quicker than

the hydrostatic equilibrium. We therefore assume the steady density structure of a non-irradiated disk in hydrostatic equilibrium calculated according to Rózańska et al. (1999). The incident flux follows a power law with $F_{inc} \propto E^{-\alpha}$, $\alpha = 0.9$ over 0.1 eV up to 100 keV. We choose a ratio $F_{inc}/F_{disk} = 144$ of incident flux of the flare to the flux coming from the disk, hence the flare by far dominates over the disk emission.

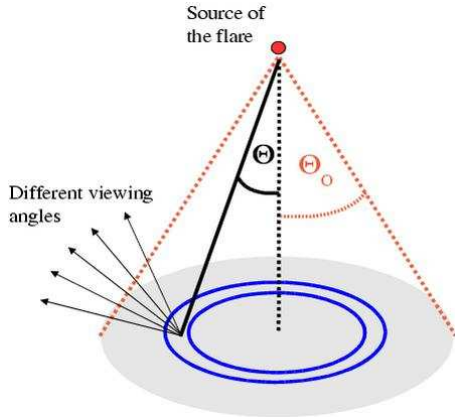


Figure 1. Flare geometry: the observed spectrum depends on the incident angle Θ of the irradiating photons and on the viewing angle. Θ_0 denotes the half-opening angle of the flare-cone.

In previous flare models the disk illumination was defined as semi-isotropic (Czerny et al. 2004; Collin et al. 2003) or with a constant incident angle (Nayakshin & Kallman 2001). However, the incident angle and the ionization parameter $\xi = \frac{4\pi F_{inc}}{n_H}$ of the flare (with F_{inc} being the incident flux and n_H being the hydrogen density at the disk surface) change significantly with the distance to the center of the illuminated spot (Fig.1). In particular we have $\xi = \xi_0(\cos\Theta)^{-3}$ if ξ_0 denotes the ionization parameter at the spot center.

We have to define a maximum radius of the irradiated spot, i.e., a maximum half-opening angle Θ_0 of the flare cone. We choose $\Theta_0 = 60^\circ$ because within the corresponding spot 50% of the luminosity reaching the disk is reprocessed. The observed reprocessed spectrum then consists of the integrated spectra of successive concentric rings at incident angles with $0^\circ < \Theta < 60^\circ$. These spectra can be computed for different inclination angles i (measured from the disk symmetry axis).

We perform detailed radiative transfer simulations coupling the codes TITAN and NOAR. TITAN simulates radiative transfer inside optically thick media (Dumont, Abrassart, & Collin 2000; Dumont et al. 2003) determining the temperature and ionization structure. NOAR is a Monte-Carlo code treating the Compton processes.

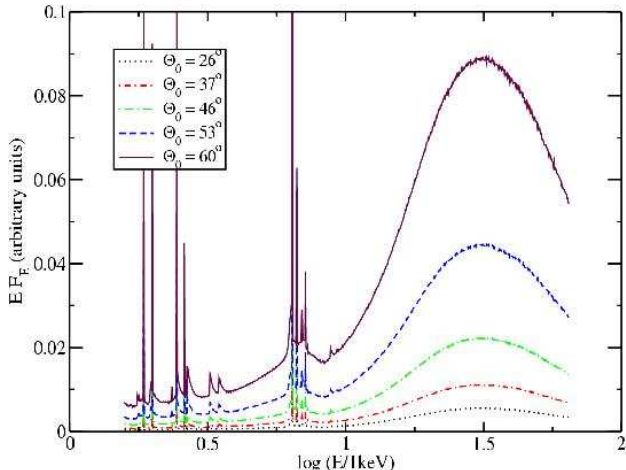


Figure 2. Integrated reflection spectra for different half-opening angles Θ_0 seen at a typical Seyfert-1 inclination $i \sim 25^\circ$; for larger half-opening angles the spectra become harder.

2.2. Results

The reflected spectra have been computed for successive rings of the illuminated hot spot up to $\Theta_0 = 60^\circ$. While the Compton hump in the hard X-ray range is rather similar for all incident angles considered, the spectral slope in the soft X-rays rises for emission regions farther away from the spot center. The integrated Compton reflection for several half-opening angles seen at an inclination of about 25° , which represents a typical Seyfert-1 inclination, are shown in Fig.2.

Due to different distances to the flare source the reprocessing will evolve in time from the center of the spot toward the outer regions. This can be seen as successively growing half-opening angles of the flare cone. The spectra should become harder as the flare intensifies. The time scale of this evolution is determined by the height of the source above the disk. Such a development was observed for the Narrow Line Seyfert 1 galaxy I Zw 1 (Gallo et al. 2004).

3. Flare-induced evolution of the disk atmosphere

After the dynamical time scale, the atmosphere settles into a new hydrostatic equilibrium with a total height H_{tot} and a Thomson optical depth τ_{es} . We constrain the effect of a flare on the total height H_{tot} and the Thomson optical depth τ_{es} .

We analytically recompute the new equilibrium and again include the angular dependence of the incident flux for different distances d from the spot center. We find the general result that the expansion of the disk atmosphere induced by the flare and its optical depth depend strongly on the distance of the flare from the central black hole.

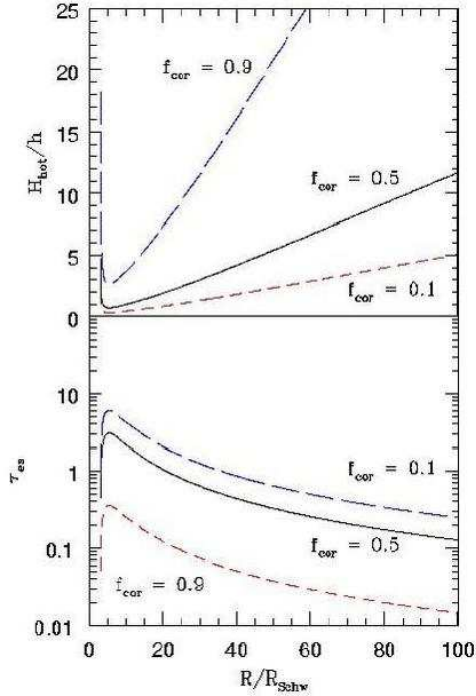


Figure 3. Top: radial dependence of the thickness (in flare height units). Bottom: Optical depth of the heated zone at the spot center. The different curves denote three values of the energy fraction f_{cor} dissipated in the corona.

In Fig.3 we show the ratio H_{tot}/h , with h being the height of the flare source, and τ_{es} versus R/R_{Schw} . We choose a black hole mass of $M = 10^8 M_{\odot}$, an accretion rate $\dot{m} = 0.03$ (Eddington units), and a covering factor of the disk surface with hot-spots of $f_{cover} = 0.1$ (see details of this work in Czerny & Goosmann (submitted)). The different curves refer to three values of the fraction of flux dissipated in the corona. The tendency in all cases is that toward the outer regions of the disk the atmosphere reaches a higher altitude and becomes optically thinner. For intermediate distances the flare source eventually will be shrouded by an optically thick ($\tau_{es} > 1$) disk atmosphere ($H_{tot}/h > 1$) which should modify the observed spectrum.

Acknowledgments. This research was supported by the CNRS No.16 ‘‘Astronomie France-Pologne’’ and by the Hans-Böckler-Stiftung.

References

- Collin, S., Coupé, S., Dumont, A.-M., Petrucci, P.-O., & Rózańska, A. 2003, A&A, 400, 437
 Dumont, A.-M., Abrassart, A., & Collin, S. 2000, A&A, 357, 823
 Dumont, A.-M., Collin, S., Paletou, F., Coupé, S., Godet, O., & Pelat, D. 2003, A&A, 407, 13

- Czerny, B., Róžańska, A., Dovčiak, M., Karas, V., & Dumont, A.-M. 2004, *A&A*, 420, 1
- Edelson, R., Turner, T. J., Pounds, K., Vaughan, S., Markowitz, A., Marshall, H., Dobbie, P., & Warwick, R. 2002, *ApJ*, 568, 610
- Gallo, L. C., Boller, T., Brandt, W. N., Fabian, A. C., & Vaughan, S. 2004, *A&A*, 417, 29
- Ponti, G., Cappi, M., Dadina, M., & Malaguti, G. 2004, *A&A*, 417, 451
- Nayakshin, S. & Kallman, T. R. 2001, *ApJ*, 546, 406
- Róžańska, A., Czerny, B., Życki, P. T., & Pojmański, G. 1999, *MNRAS*, 305, 481
- Vaughan, S. & Fabian, A. C. 2004, *MNRAS*, 348, 1415